Electronic States of a Single Layer of Pentacene: Standing-Up and Flat-Lying Configurations†

Maria Grazia Betti,*,‡ Aloke Kanjilal,‡,£ and Carlo Mariani‡

Dipartimento di Fisica, Università di Roma "La Sapienza", Piazzale Aldo Moro 2, I-00185 Roma, Italy, and INFM-CNR Center on nanoStructures and bioSystems at Surfaces (S^3), Via G. Campi 231/A, I-41100 Modena, Italy

Received: June 6, 2007; In Final Form: August 3, 2007

The electronic properties of a single layer (SL) of pentacene molecules are investigated by high-resolution UV photoemission and near-edge X-ray absorption spectroscopy in different configurations of the SL, either standing up on an aromatic self-assembled monolayer or planar on a bare Cu(001) substrate. The weakly interacting pentacene molecules in the standing-up SL present a semiconducting character, and the empty states distribution reflects that of gas-phase pentacene, while the planar pentacene−Cu system shows a metallic interface with redistribution of the empty molecular states. The highest-occupied molecular orbital lineshape in the weakly interacting SL shows a double structure, attributed to two nonequivalent molecules in the ordered configuration.

Introduction

In the rapidly expanding field of the electronics based on hybrid organic−inorganic systems, the design of new architectures of π-conjugated materials has stimulated an enormous interest in realizing prototype hybrid organic devices,[1−6] where the performance and success depend mainly on the molecular orientation and packing.[2,3,7−9] Recently, a high-mobility and low-voltage organic thin-film transistor (TFT) has been designed with a heterostructure constituted of standing-up pentacene molecules deposited on a buffer self-assembled monolayer (SAM), where the SAM has been used successfully as a dielectric layer instead of a thin oxide for reducing the operating voltages.[10−14] Pentacene ($C_{22}H_{14}$) presents electron charge delocalized on the fused benzene rings supported by a highest-occupied molecular orbital (HOMO) and a lowest-unoccupied molecular orbital (LUMO). Taking into account the pentacene polymorphs[15,16] or other nanostructured architectures or single-layer (SL) phases[17] due to the different packing of pentacene molecules, the carrier mobility is basically governed by the strength of the electronic coupling between the HOMO levels (for hole transport) and the LUMO states (for electron transport) of adjacent molecules in a band-transport mechanism,[18,19] where the transfer integral (electronic coupling) has generally been invoked to quantify the mechanism.[19,20]

The pentacene orientation and the molecule−substrate interaction are crucial to understand the related electronic and transport properties of the organic devices. With the aim of studying those mechanisms that tune the transport properties of organic/inorganic interfaces, we have separately prepared ordered single layers of standing-up and flat-lying pentacene arrays, respectively, and measured and compared the molecular electronic states supporting the mobile charge carriers in the two structural configurations. The main objective is to clarify to what extent the HOMO and LUMO states are involved in the molecule−molecule and molecule−substrate interactions. Pentacene can be adsorbed as a single layer of standing-up molecules on a buffer SAM of benzenethiolate (C_6H_5S-, Bt) or a SL of flat-lying molecules directly on a bare Cu surface, as deduced by near-edge X-ray absorption fine structure (NEXAFS) at the C K-edge. While a SL of standing-up molecules weakly interacts with the underlying SAM, the strong redistribution of the LUMO-related final states for flat-lying pentacene on Cu is a sign of an electronic mixing between the molecular orbitals and the metal electronic states. The latter phenomenon can be accounted for by considering a partial LUMO occupation induced by the metal charge, enhancing the metallic character at the interface. This process can largely influence the charge injection barrier and the device performance. On the other side, the electronic-transport properties of the pentacene SL deposited on the SAM buffer are not affected by the substrate and preserve the semiconducting properties due to the $\pi-\pi$ interaction of the pentacene standing-up floating layer.

Experimental Section

The HR-ARUPS experiments were performed at the LOTUS laboratory in Rome, in an ultrahigh-vacuum (UHV, base pressure 10^{-8} Pa) environment. Details of the experimental approach have been given elsewhere.[13] HR-ARUPS data were acquired using a high-intensity He discharge lamp (He I_α photons, $h\nu = 21.218$ eV) with a 45° incidence angle, and the photoemitted electrons were analyzed in the plane of incidence with a hemispherical SCIENTA SES-200 analyzer, used with an energy resolution of 15 meV and an angular resolution of 0.18° and by keeping the integration angle of ± 8° with respect to the direction of normal emission for the angle-integrated measurements. The Cu(001) and Cu(119) single crystals were cleaned by repeated sputtering−annealing cycles,[13,21] and the Cu(001) was exposed to benzenethiol (C_6H_5SH) vapors in UHV

† Part of the "Giacinto Scoles Festschrift".

* To whom correspondence should be addressed. Phone: +39 06 49914389. Fax: +39 06 4957697. E-mail: betti@roma1.infn.it.

‡ Università di Roma "La Sapienza".

£ INFM-CNR Center on nanoStructures and bioSystems at Surfaces (S^3).

10.1021/jp074365i CCC: $37.00
Published on Web 11/08/2007

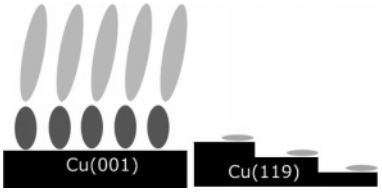

Figure 1. Left: schematic side-view of the arrangement of standing-up pentacene molecules in the SL phase on the Bt-SAM/Cu(001) substrate.[13] Right: schematic side view of the flat-lying pentacene molecules on the Cu(119) surface, where the SL pentacene molecules are lying flat along the step edges.[21]

to prepare the saturated Bt-SAM.[13] Pentacene was evaporated in situ at 300 K with a constant evaporation rate of about 1 nm/min.

Another set of samples was prepared with the same procedures and measured at the ALOISA beamline[22] of the Elettra Synchrotron Radiation Laboratory (Trieste, Italy). Photon energy scans from 275 to 320 eV with a photon energy resolution of 100 meV were carried out during NEXAFS measurements at the C K-edge. The NEXAFS signal was measured by means of an electron multiplier facing the sample, operated with a −200 V biased grid.[23,24] These configurations were achieved in the specific experimental setup of the ALOISA beamline by rotating the sample around the axis coincident with the X-ray beam, keeping the X-ray incidence angle fixed at 83°.

Results and Discussion

A SL of standing-up pentacene is formed by depositing 20 Å (nominal thickness) of pentacene on Bt-SAM/Cu(001), while a SL of flat-lying molecules is formed by adsorbing 3 Å of pentacene on the Cu(119) surface, as previously deduced by atomic force microscopy (AFM)[13] and scanning tunneling microscopy (STM).[21,25,26] A schematic drawing of the pentacene SL standing up on the Bt-SAM and lying flat on the Cu(119) vicinal surface is reported in Figure 1. The step edges of the Cu(119) vicinal surface, with 1.17 nm wide terraces, provide ideal adsorption sites for producing long-range ordered pentacene arrays lying flat along the step edges, as observed by STM.[21,25] On the other hand, the Bt-SAM induces a standing-up configuration of the pentacene SL, as deduced by the average layer thickness recently measured by AFM.[13]

The molecular geometry and the evolution of the molecular states for pentacene SLs deposited on both substrates have been investigated by NEXAFS at the C K-edge. The polarization-dependent C K-shell spectra for the SL-pentacene/Bt-SAM/Cu(001) and SL-pentacene/Cu(001) systems are shown in Figure 2. NEXAFS spectra were collected as a function of the polar angle between the X-ray scattering plane and the photon electric field vector (***E***), ranging between s and p polarization, respectively: ***E*** perpendicular to the scattering plane and parallel to the substrate (s polarization), or ***E*** parallel to the scattering plane and perpendicular to the substrate (p polarization). The absorption peaks can be assigned to the transitions from the C 1s core level to the π^* molecular states (280−290 eV energy range) and to the σ^* resonances (at higher energy). In particular, there is a strong dichroism for s- and p-polarized radiation, though it is reversed for the two systems. For pentacene on the bare Cu(001) surface (Figure 2, top panel), the signal in the π^* region is enhanced for p-polarized radiation as compared to that with the s-polarized one, with reversed behavior for the σ^* resonance. In the pentacene/Bt-SAM/Cu(001) system (Figure 2, bottom panel), the π^* resonances are more intense for s-polarized radiation as compared with that for p polarization. Due to the

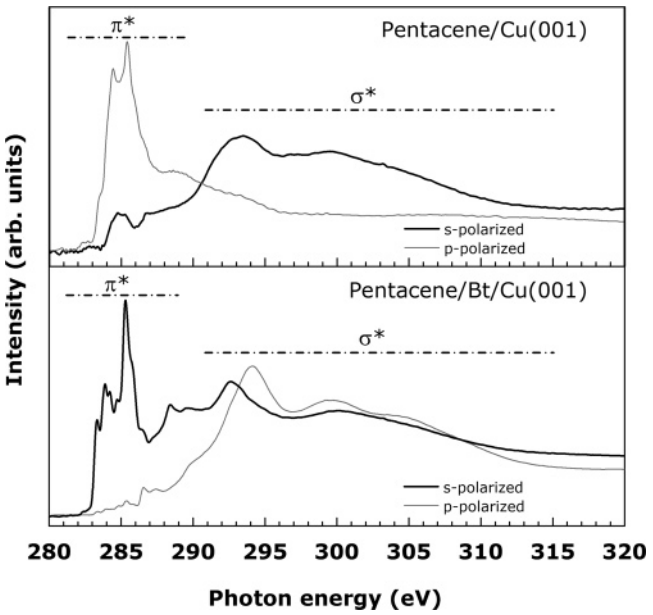

Figure 2. Top panel: C K-edge NEXAFS absorption spectra of 6 Å of pentacene deposited on the Cu(001) surface for both s-polarized (black solid line) and p-polarized (gray solid line) radiation. Bottom panel: C K-edge NEXAFS absorption spectra of a 20 Å pentacene/Bt-SAM/Cu(001) system for both s-polarized (black solid line) and p-polarized (gray solid line) radiation.

observed C K-shell dichroism and to the orbital symmetry of the π^* states, we can unambiguously confirm that pentacene molecules adsorbed on the organic Bt-SAM adopt the standing-up configuration, in agreement with a previous AFM study,[13] while pentacene is lying flat when adsorbed on the bare Cu(001) substrate, as it does on its vicinal (119) surface[27] (in agreement with STM results[25]).

More details on the nature of molecule−substrate and molecule−molecule interactions can be deduced by comparing the C K-edge line shapes. The C K-edge absorption line shape for a SL of standing-up pentacene molecules deposited on the SAM is very close to that obtained for gas-phase pentacene,[28] and this similarity is maintained at lower nominal pentacene thickness, signifying a weak molecule−substrate interaction at any pentacene coverage on the Bt-SAM. In particular, there are two main manifolds in the π^* energy region (282−284.5 and 284.5−287 eV, respectively) due to the absorption from the C 1s core levels to the LUMO and LUMO+1 states. The fine structure within each manifold reflects the slightly different initial state energy of the six nonequivalent C atoms involved in the transitions, as detailed by a previous gas-phase data analysis.[28] Further fine structure in the $\pi^* + \sigma^*$ region (287.5−291.5 eV) is absent in the gas-phase data,[28] and it can be attributed to mixed orbitals due to the molecule−molecule interaction within the SL. On the other hand, a closer inspection of the line shape for the NEXAFS data at the pentacene/Cu(001) system reveals a definitely modified line shape in the π^*-transition region, with respect to the pentacene/Bt spectra and to the free-molecule data.[28] The two manifolds in the π^* energy region are not any more clearly resolved, and the dichroism in the signal is apparently reduced. These effects are due to molecule−substrate interaction at the Cu(001) substrate, producing a modification of the empty final states accessed by the core electrons, as invoked previously for the pentacene/Cu(119) interface,[27] with hybridization between the molecular orbitals and the metal electronic states. In fact, recent theoretical predictions[29] and experimental photoemission results[29,30] reveal hybridization of the π^* molecular orbitals with the underlying

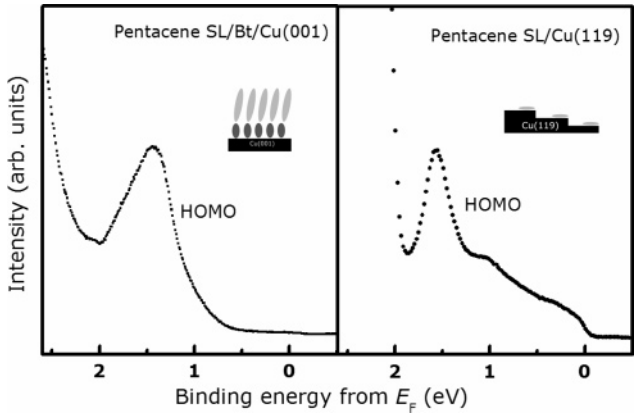

Figure 3. Left panel: HR-UPS spectrum of 20 Å pentacene/Bt-SAM/Cu(001) taken at normal emission. Right panel: HR-UPS spectrum of 3 Å pentacene/Cu(119) taken at 60° out of normal emission (to enhance surface sensitivity). In the insets are schematic views of the two molecular configurations.

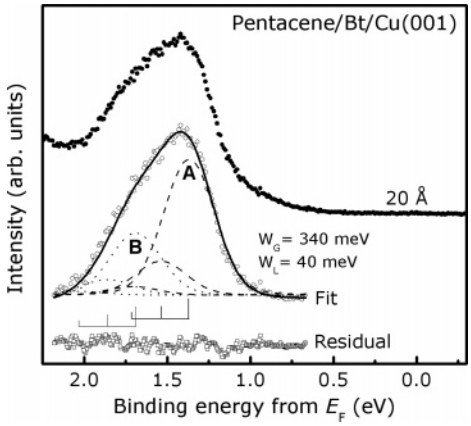

Figure 4. HR-UPS data for the 20 Å pentacene/Bt-SAM/Cu(001) system in the HOMO binding energy region (filled circles, top spectrum). Data are after background subtraction (open circles, middle spectrum), and fitting curves (black solid line) with the residual signal (open square, at the bottom). The individual fitting curves due to the hole−vibration coupling for bands A (dashed lines) and B (dotted lines) are superimposed on the background-subtracted experimental data, and their positions are marked by schematic combs associated to the excitations A and B.

metallic states, inducing partial occupation of the former LUMO molecular states. This scenario is consistent with a decreasing of the LUMO component and a redistribution of the LUMO+1 states in the C K-edge for the flat-lying pentacene molecules (Figure 2, top panel). In conclusion, the molecule−metal interaction strongly influences the energy distribution of the LUMO molecular states in the interaction with the Cu surface, while the standing-up pentacene layer is floating on the SAM buffer layer and the LUMO states are preserved, reflecting the energy distribution similar to the one as reported for the gas phase.[28]

A study for obtaining the exact angle in the molecular orientation can be obtained only after a very accurate theoretical prediction of the different spectral contributions upon molecule adsorption/interaction on the substrate, which cannot be directly related to the gas-phase molecular peaks.

Further insights on the electronic properties of these single arrays of standing-up and flat-lying pentacene molecules can be deduced by comparing the HOMO-derived states. High-resolution UPS data in the HOMO energy region for a 20 Å thick pentacene layer deposited on the Bt-SAM/Cu(001) system and on a 3 Å thick pentacene layer deposited on the bare Cu(119) surface are shown in Figure 3. The pentacene SL grown on the Bt-SAM (Figure 3, left panel) is semiconducting, as documented by the absence of electronic spectral density at the Fermi energy (E_F), and the hole-injection barrier (ϕ_h) is estimated to be 1.00 ± 0.05 eV. On the other hand, the SL pentacene/Cu(119) system (Figure 1, right panel) presents a finite density of states at E_F due to partial occupation of the LUMO, confirming the metallic character at the interface, as predicted by theoretical calculations.[29]

The metallic pentacene/Cu(119) interface presents a narrow (0.3 eV) and symmetric HOMO structure centered at a 1.57 eV binding energy (BE), while the pentacene/Bt-SAM presents an asymmetric HOMO band (0.6 eV wide) centered at a 1.44 eV BE. The symmetric line shape at the metallic interface is due to the complete screening of hole−vibrational coupling, which is present for the pentacene HOMO in the gas phase.[25,31] The HOMO asymmetry in the standing-up pentacene SL is due to the presence of a double structure, reported in Figure 4 (top spectrum) along with the results of a fitting procedure, using Voigt functions. A fit with a single excitation mode followed by hole−vibration couplings (C−C stretching mode at 170 meV[25,31−33] and higher-order loss peak, as reported for gas-phase pentacene[25,31]) was not successful. Thus, we introduced two electronic components (A and B), each accompanied by a series of hole−vibration couplings, as shown in Figure 4 (lower spectrum), with full-width at half-maximum (fwhm) values of the Gaussian (W_G) and Lorentzian (W_L) components of 340 and 40 meV, respectively.[34] The two main electronic excitations (A and B) centered at the 1.37 and 1.70 eV BEs, respectively, are always present at different pentacene thicknesses on the Bt-SAM buffer layer.

In recent works on pentacene thin films adsorbed on weakly interacting substrates, the appearance of asymmetric HOMO peaks[12,15,25,32,33,35,36] has been attributed either to the contribution of bulk and surface components[25,33,37] and/or to the energy band dispersion,[32,35,38,39] with a bandwidth of 0.19 eV at room temperature.[35] Thus, we performed an angular-resolved photoemission study of the SL pentacene deposited on the Bt-SAM/Cu(001) and on the Cu(119) vicinal surface, along the $\bar{\Gamma}\bar{X}$ direction of the (1 × 1) surface brillouin zone (SBZ) of the metal substrate. The HR-ARUPS spectra present a HOMO double peak well localized over the SBZ spanning along $\bar{\Gamma}\bar{X}$ for the pentacene SL on the Bt-SAM. In particular, its double-peaked shape does not change in any point of that symmetry direction, discarding the possibility to justify the double-peaked HOMO structure as purely due to energy band dispersion. We cannot exclude the possibility that some dispersion may be present in another symmetry direction or thin-film configuration;[40] however, the negligible bandwidth for the floating pentacene SL confirms that the molecular states are weakly effected by the environment. On the other side, preliminary observation of a tiny dispersion (about 0.1 eV) is obtained for the SL deposited on the Cu(119) surface, where the molecular levels do interact with the underlying metallic electronic states; electronic mixing between the pentacene molecular orbitals and the electronic states at the Cu(001) surface has been recently demonstrated by a joint theoretical and experimental approach, observing a redistribution of states close to the Fermi energy.[29] Thus, the metallic substrate mediates the molecule−molecule interaction, as recently discussed for other π-conjugated molecules interacting on a silver surface,[41] producing a non-negligible bandwidth for the pentacene SL on Cu(119), which can influence the charge mobility at the interface.

The asymmetry of the HOMO structure for the floating pentacene layer observed for a SL and for a lower nominal

thickness cannot be ascribed to the coexistence of surface and bulk components. A SL of standing-up molecules deposited on Bt-SAM/Cu(001) provides a well-ordered two-domain $c(2 \times 6)$ phase at low coverage,[42] though a loss of azimuthal ordering is observed at increasing molecular density.[13] Considering almost vertical alignment of the pentacene molecules on the Bt-SAM/Cu(001), we can suppose that each molecule is adsorbed standing up on each underlying Bt molecule in the $c(2 \times 6)$ sites of the Cu(001) surface, giving rise to a structure with two molecules per surface unit cell. Hence, we may attribute the double-HOMO structure to the presence of two nonequivalent molecules in the surface unit cell, as proposed in theoretical predictions.[19,20,43−45] Generally, absorption of radiation in such a low-symmetry situation produces two different absorption bands, as originally predicted by Davydov[46] and observed in optical[47,48] and absorption[49] measurements. Despite the weak interaction of pentacene with the Bt-SAM substrate, the presence of two nonequivalent molecules and their mutual interaction may lead to a kind of Davydov/crystal-field splitting of the initial state, giving rise to the observed 0.33 eV energy splitting of the corresponding HOMO bands.

Conclusions

In conclusion, we presented a comparison of the electronic properties of a single layer of pentacene molecules arranged on an organic SAM and on a bare Cu metal substrate by means of combined high-resolution ARUPS and NEXAFS measurements. Pentacene adsorbs in a standing-up orientation on the weakly interacting SAM, while the molecules are lying flat on the bare Cu(001) substrate. The floating 2D pentacene layer on the SAM has a semiconducting character with a double-HOMO structure, justified by the $c(2 \times 6)$ adsorption geometry. The flat-lying 2D pentacene layer on Cu interacts with the underlying metal, giving rise to a metallic interface with a redistribution of the empty molecular states.

Acknowledgment. This work is partially funded by grants of Roma "La Sapienza" University. Experimental assistance by M. Beccari and by the ALOISA beamline staff at Elettra (Trieste) is gratefully acknowledged.

References and Notes

(1) Ishii, H.; Sugiyama, K.; Ito, E.; Seki, K. *Adv. Mater.* **1999**, *11*, 605.
(2) Dimitrakopoulos, C. D.; Malenfant, P. R. L. *Adv. Mater.* **2002**, *14*, 99.
(3) Karl, N. *Synth. Met.* **2003**, *133−134*, 649.
(4) Jang, J. *Mater. Today* **2006**, *9*, 46.
(5) Toccoli, T.; Pallaoro, A.; Coppedè, N.; Iannotta, S.; De Angelis, F.; Mariucci, L.; Fortunato, G. *Appl. Phys. Lett.* **2006**, *88*, 132106.
(6) De Angelis, F.; Cipolloni, S.; Mariucci, L.; Fortunato, G. *Appl. Phys. Lett.* **2006**, *88*, 193508.
(7) Casalis, L.; Danisman, M. F.; Nickel, B.; Bracco, G.; Toccoli, T.; Iannotta, S.; Scoles, G. *Phys. Rev. Lett.* **2003**, *90*, 206101.
(8) Jurchescu, O. D.; Baas, J.; Palstra, T. T. M. *Appl. Phys. Lett.* **2004**, *84*, 3061.
(9) Witte, G.; Wöll, C. *J. Mater. Res.* **2004**, *19*, 1889.
(10) Bock, C.; Pham, D. V.; Kunze, U.; Käfer, D.; Witte, G.; Wöll, Ch. *J. Appl. Phys.* **2006**, *100*, 114517.
(11) Hu, W. S.; Tao, Y. T.; Hsu, Y. J.; Wei, D. H.; Wu, Y. S. *Langmuir* **2005**, *21*, 2260.
(12) Ihm, K.; Kim, B.; Kang, T.-H.; Kim, K.-J.; Joo, M. H.; Kim, T. H.; Yoon, S. S.; Chung, S. *Appl. Phys. Lett.* **2006**, *89*, 033504.
(13) Kanjilal, A.; Ottaviano, L.; Di Castro, V.; Beccari, M.; Betti, M. G.; Mariani, C. *J. Phys. Chem. C* **2007**, *111*, 286.
(14) Kang, J. H.; da Silva Filho, D.; Brédas, J. L.; Zhu, X.-Y. *Appl. Phys. Lett.* **2005**, *86*, 152115.
(15) Mattheus, C. C.; de Wijs, G. A.; de Groot, R. A.; Palstra, T. T. M. *J. Am. Chem. Soc.* **2003**, *125*, 6323.
(16) Mattheus, C. C.; Dros, A. B.; Baas, J.; Meetsma, A.; de Boer, J. L.; Palstra, T. T. M. *Acta Crystallogr., Sect. C* **2001**, *57*, 939.
(17) Fritz, S. E.; Martin, S. M.; Frisbie, C. D.; Ward, M. D.; Toney, M. F. *J. Am. Chem. Soc.* **2004**, *126*, 4084.
(18) Cornil, J.; Beljonne, D.; Calbert, J.-P.; Brédas, J. L. *Adv. Mater.* **2001**, *13*, 1053.
(19) Cheng, Y. C.; Silbey, R. J.; da Silva Filho, D. A.; Calbert, J. P.; Cornil, J.; Brédas, J. L. *J. Chem. Phys.* **2003**, *118*, 3764.
(20) Valeev, E. F.; Coropceanu, V.; da Silva Filho, D. A.; Salman, S.; Brédas, J. L. *J. Am. Chem. Soc.* **2006**, *128*, 9882.
(21) Gavioli, L.; Fanetti, M.; Sancrotti, M.; Betti, M. G. *Phys. Rev. B* **2005**, *72*, 035458.
(22) Details of the ALOISA beamline can be found at http://www.elettra.trieste.it/experiments/beamlines/aloisa/index.html.
(23) Gotter, R.; Ruocco, A.; Morgante, A.; Cvetko, D.; Floreano, L.; Tommasini, F.; Stefani, G. *Nucl. Instrum. Methods Phys. Res., Sect. A* **2001**, *467−468*, 1468.
(24) Cossaro, A.; Cvetko, D.; Bavdek, G.; Floreano, L.; Gotter, R.; Morgante, A.; Evangelistra, F.; Ruocco, A. *J. Phys. Chem. B* **2004**, *108*, 14671.
(25) Baldacchini, C.; Mariani, C.; Betti, M. G.; Gavioli, L.; Fanetti, M.; Sancrotti, M. *Appl. Phys. Lett.* **2006**, *89*, 152119.
(26) Baldacchini, C.; Betti, M. G.; Corradini, V.; Mariani, C. *Surf. Sci.* **2004**, *566−568*, 613.
(27) Baldacchini, C.; Allegretti, F.; Gunnella, R.; Betti, M. G. *Surf. Sci.* **2007**, *601*, 2603.
(28) Alagia, M.; Baldacchini, C.; Betti, M. G.; Bussolotti, F.; Carravetta, V.; Ekström, U.; Mariani, C.; Stranges, S. *J. Chem. Phys.* **2005**, *122*, 124305.
(29) Ferretti, A.; Calzolari, A.; Di Felice, R.; Ruini, A.; Molinari, E.; Baldacchini, C.; Betti, M. G. *Phys. Rev. Lett.* **2007**, *99*, 046802.
(30) Baldacchini, C.; Mariani, C.; Betti, M. G. *J. Chem. Phys.* **2006**, *124*, 154702.
(31) Coropceanu, V.; Malagoli, M.; da Silva Filho, D. A.; Gruhn, N. E.; Bill, T. G.; Brédas, J. L. *Phys. Rev. Lett.* **2002**, *89*, 275503.
(32) Fukagawa, H.; Yamane, H.; Kataoka, T.; Kera, S.; Nakamura, M.; Kudo, K.; Ueno, N. *Phys. Rev. B* **2006**, *73*, 245310.
(33) Harada, Y.; Ozaki, H.; Ohno, K. *Phys. Rev. Lett.* **1984**, *52*, 2269.
(34) Yamane, H.; Nagamatsu, S.; Fukagawa, H.; Kera, S.; Friendlein, R.; Okudaira, K. K.; Ueno, N. *Phys. Rev. B* **2005**, *72*, 153412.
(35) Koch, N.; Vollmer, A.; Salzmann, I.; Nickel, B.; Weiss, H.; Rabe, J. P. *Phys. Rev. Lett.* **2006**, *96*, 156803.
(36) Weng, S.-Z.; Hu, W.-S.; Kuo, C.-H.; Tao, Y.-T.; Fan, L.-J.; Yang, Y.-W. *Appl. Phys. Lett.* **2006**, *89*, 172103.
(37) Salaneck, W. R. *Phys. Rev. Lett.* **1978**, *40*, 60.
(38) Yamane, H.; Kera, S.; Yoshimura, D.; Okudaira, K. K.; Seki, K.; Ueno, N. *Phys. Rev. B* **2003**, *68*, 033102.
(39) Hasegawa, S.; Mori, T.; Imaeda, K.; Tanaka, S.; Yamashita, Y.; Inokuchi, H.; Fujimoto, H.; Seki, K.; Ueno, N. *J. Chem. Phys.* **1994**, *100*, 6969.
(40) Kakuta, H.; Hirahara, T.; Matsuda, I.; Nagao, T.; Hasegawa, S.; Ueno, N.; Sakamoto, K. *Phys. Rev. Lett.* **2007**, *98*, 247601.
(41) Temirov, R.; Soubatch, S.; Luican, A.; Tautz, F. S. *Nature* **2006**, *444*, 350.
(42) Kanjilal, A.; Bussolotti, F.; Crispoldi, F.; Beccari, M.; Di Castro, V.; Betti, M. G.; Mariani, C. *J. Phys. IV* **2006**, *132*, 301.
(43) Deng, W.-Q.; Goddard, W. A., III *J. Phys. Chem. B* **2004**, *108*, 8614.
(44) Northrup, J. E.; Tiago, M. L.; Louie, S. G. *Phys. Rev. B* **2002**, *66*, 121404.
(45) Tiago, M. L.; Northrup, J. E.; Louie, S. G. *Phys. Rev. B* **2005**, *67*, 115212.
(46) Davydov, A. S. In *Theory of Molecular Excitons*, translated by Kasha M., Oppenheimer J.; Series in Advanced Chemistry; McGraw-Hill: New York, 1962; p 79.
(47) Cazayous, M.; Sacuto, A.; Horowitz, G.; Lang, Ph.; Zimmers, A.; Lobo, R. P. S. M. *Phys. Rev. B* **2004**, *70*, 081309(R).
(48) He, R.; Tassi, N. G.; Blanchet, G. B.; Pinczuk, A. *Appl. Phys. Lett.* **2005**, *87*, 103107.
(49) Schuster, R.; Knupfer, M.; Berger, H. *Phys. Rev. Lett.* **2007**, *98*, 037402.